

Wavevector-dependent quantum-size effect in electron decay length at Pb thin film surfaces

Xin Liu,^{1,2} S. B. Zhang,³ X. C. Ma,⁴ Jin-Feng Jia,⁵ Qi-Kun Xue,⁵ Xin-He Bao,¹ and Wei-Xue Li^{1,a)}

¹State Key Laboratory of Catalysis, Dalian Institute of Chemical Physics, Chinese Academy of Sciences, Dalian 116023, People's Republic of China

²Department of Chemistry, Dalian University of Technology, Dalian 116024, People's Republic of China

³Department of Physics, Applied Physics, and Astronomy, Rensselaer Polytechnic Institute, Troy, New York 12180, USA

⁴Institute of Physics, Chinese Academy of Sciences, Beijing 100190, People's Republic of China

⁵Department of Physics, Tsinghua University, Beijing 100084, People's Republic of China

(Received 17 May 2008; accepted 11 August 2008; published online 3 September 2008)

The physical origin of quantum-size effects (QSEs) and its impact on the decay length of electrons in Pb thin films are studied by first-principles calculations. We show that QSE is not only size but also wavevector dependent: being maximum at $\bar{\Gamma}$ due to strong interlayer coupling between p_z orbitals, but could be vanishingly small at other symmetry points due to weak interlayer coupling between $p_{x,y}$ orbitals. The electron decay length also exhibits systematic oscillations with film thickness and the $\bar{\Gamma}$ valley has the slowest decay. © 2008 American Institute of Physics. [DOI: 10.1063/1.2977529]

For decades, quantum-size effects (QSE) have dominated the study of nanoscience, especially the structural stability and electronic properties of nanomaterials.^{1–11} The physics of the QSE is rather straightforward, namely, the finite size of a system causes a quantization of the kinetic energy, which manifests itself as distinct peaks in the density of states (DOS) or quantum well states (QWS). The formation and the existence of the QWS on atomically flat metal ultrathin films at different thicknesses have been identified and probed by using photoemission spectroscopy,¹² density functional theory (DFT) calculations,¹³ and scanning tunneling spectroscopy (STS).^{14–16} Recently, QWS for atomically flat Pb(111) mesas, fabricated on top of stepped Si(111)–(7×7) substrate, have been identified^{14,15} by taking the current-voltage differential (dI/dV), and the local work function (LWF) has been measured by using STS.¹⁶ Surprisingly, the STS-measured LWF showed remarkable quantum oscillation as a function of the film thickness N , where the oscillation of the LWF can be as large as 100 meV even when $N=35$ ML. This is at least one order of magnitude larger than the previous calculated work function,¹³ for which the variation is already less than 10 meV for $N=24$ ML. In addition, there is a one-to-one correspondence and same beating pattern at 18 ML between the LWF and the measured QWS, not seen in Ref. 13.

To understand these findings, we have carried out extensive DFT calculations for electronic states at different k -points of the surface Brillouin zone (SBZ) for Pb(111) films with N ranging from 4 to 24 ML. Our in-depth analysis reveals that the quantization of the electronic states, which results in the formation of QWS, mainly takes place at around the SBZ center, i.e., the $\bar{\Gamma}$ valley. We found that the decay of the $\bar{\Gamma}$ valley states (derived from the interlayer coupling of the p_z orbitals) is much slower due to strong inter-

layer coupling between p_z orbitals than any other states far away from the $\bar{\Gamma}$ valley (derived mainly from the in-plane $p_{x,y}$ orbitals) due to weak interlayer coupling between $p_{x,y}$ orbitals. Further analysis showed that the decay of the electronic states at $\bar{\Gamma}$, in contrast to the overall charge density, presents significant QSE. The slow decaying $\bar{\Gamma}$ states would be first picked up during the STS measurements, which account for the one-to-one correspondence and same beating pattern between the LWF and the QWS.

Our calculations use the ultrasoft pseudopotential plane wave codes.¹⁷ We expanded the Kohn–Sham wave functions in the plane wave basis set with $E_{\text{cut}}=25$ Ry, and the PW91 functional¹⁸ for exchange correlation. The SBZ sampling was carried out with Monkhorst–Pack ($13 \times 13 \times 1$) grid.¹⁹ The Pb(111) films were simulated as slabs inside supercells at optimized bulk lattice constant of 5.03 Å, and the top five layers were fully relaxed. The length of the supercells was fixed at 107 Å. The smallest vacuum region was 30 Å for the thickest 24 ML film. The effects of silicon substrates were studied by placing Pb(111)(2×2) films on five layers Si(111)–($\sqrt{3} \times \sqrt{3}$) with hydrogen passivation at the bottom. The corresponding SBZ was sampled by the Monkhorst–Pack ($7 \times 7 \times 1$) grid.¹¹

Figure 1(a) shows the band structure of a typical 8 ML Pb(111) film. We note that (1) the energy minima of the $6p$ states reside at symmetry points $\bar{\Gamma}$ and \bar{M} . At the $\bar{\Gamma}$ valley well separated subbands in the energy range from -4 to $+1$ eV with upward parabolic dispersions are readily seen. (2) Between symmetry points, two bands from adjacent valleys cross each other, for instance, at the $\bar{\Sigma}$ point. Orbital projected local DOS (not plotted) shows that the occupied p bands around the $\bar{\Gamma}$ valley are mainly from the $6p_z$ orbital, whereas the occupied p bands around the \bar{M} valleys are mainly from the $6p_{x,y}$ orbital. The different size dependences of the QWS at different k -points of the SBZ are reflected in

^{a)}Electronic mail: wxli@dicp.ac.cn.

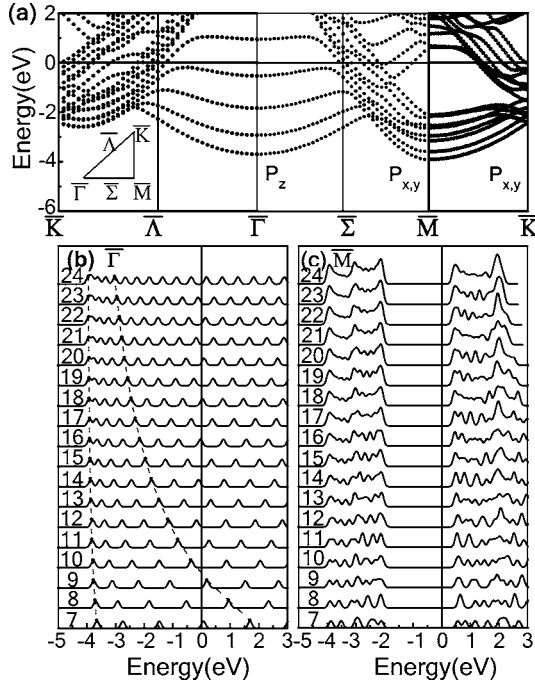


FIG. 1. (a) Surface band structure of an 8 ML Pb(111) film. Energy zero is at the Fermi level, and the symmetry of the atomic states are identified as $6p_z$ and $6p_{x,y}$. (b) and (c) are k -point resolved DOS at $\bar{\Gamma}$ and \bar{M} , respectively.

the calculated DOS (with broadening factor 0.1 eV) in Figs. 1(b) and 1(c). The DOS ($\bar{\Gamma}$) in Fig. 1(b) further shows how the QWS made of p_z states evolve, over a wide range of N from 7 to 24 ML. When increasing N , all QWS move downward; empty QWSs move down below the E_F to become occupied. Any state in the $\bar{\Gamma}$ valley can be described in a similar manner. In contrast the DOS (\bar{M}) shows little sign of QSE.

One can qualitatively understand these results as follows. The \bar{M} states are the $p_{x,y}$ states. Naturally, they couple strongly in plane parallel to the surface, but only weakly between planes. In a simple nearest-neighbor tight-binding picture, this means that the interlayer coupling $U^z = \langle p_{x,y} | V(\vec{r}) | \bar{p}_{x,y} \rangle$ is considerably smaller than the intralayer coupling $U^{x,y} = \langle p'_{x,y} | V(\vec{r}) | p''_{x,y} \rangle$. Consequently, QSE due to the removal of the adjacent layers is small. In comparison, the $\bar{\Gamma}$ states are p_z states for which interlayer $V^z = \langle p_z | V(\vec{r}) | \bar{p}_z \rangle$ is considerably larger than intralayer $V^{x,y} = \langle p'_z | V(\vec{r}) | p''_z \rangle$. Consequently, QSE due to layer removal is also large.

The existence of the QWS has been identified by STS dI/dV measurement.¹⁴ Because the decay of the surface electron density directly impacts the electron tunneling rate,⁵ we have studied the spatial decay of the electron states. The decay is quantified by fitting the electronic state in Fig. 2(a) with an exponential function $\rho(z) = \rho^0 \text{Exp}(-z/\lambda)$, where the decay length λ is the inverse of the slope in the natural logarithmic plot. Figure 2(a) shows the representative results for $N=8$ ML for highest occupied QWS (HOQWS) over the entire SBZ and in the energy range from -4 to 0 eV ($=E_F$). The results reveal that the spatial decay of the $\bar{\Gamma}$ states is considerably slower than any other states. Our calculated λ s are 0.54, 0.39, and 0.33 Å for the HOQWS at $\bar{\Gamma}$, $\bar{\Lambda}$, and \bar{M} , respectively. In terms of charge density, ρ at $\bar{\Gamma}$ is a factor of

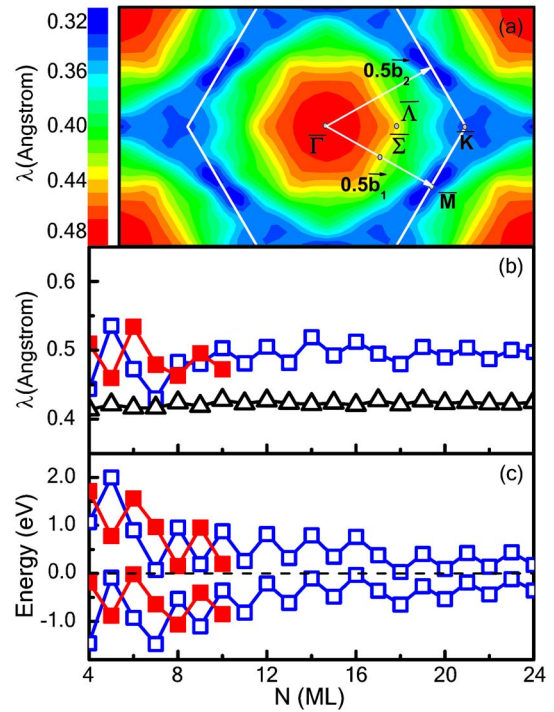


FIG. 2. (Color online) (a) Calculated decay length over the entire SBZ for states from 4 eV below to the Fermi level. $N=8$ ML. (b) Calculated decay length at $\bar{\Gamma}$ for free standing (open squares) and Si-supported (solid squares) Pb films, and from the overall charge density for the free standing films (triangular) as a function of N . (c) Calculated HOQWS and LUQWS, as a function of N . Legends are the same as in (b).

10 larger than those at $\bar{\Lambda}$ and \bar{M} at a typical $z=4$ Å.

To qualitatively understand the symmetry-dependent decay lengths in Fig. 2, we again resort to the simple tight-binding model. Basically, for the non- $\bar{\Gamma}$ states with $U^z \ll U^{x,y}$ coupling between $p_{x,y}$ states at the surface layer and $p_{x,y}$ states in the virtual layers outside the surface is small. For the $\bar{\Gamma}$ states, however, because $V^z \gg V^{x,y}$, coupling between p_z states at the surface layer and p_z states in the virtual layers is significantly larger. Thus, more virtual orbitals will be required in order to make a smooth transition from bulk to vacuum, resulting in a longer decay length.

Figure 2(b) shows oscillation features of the decay length at $\bar{\Gamma}$ as a function of N obtained for the Pb layers with and without the Si substrate, while Fig. 2(c) shows those for HOQWS and lowest unoccupied QWS (LUQWS). We see that both the calculated λ [open squares in Fig. 2(b)] and the QWS [Fig. 2(c)] exhibit the even-odd oscillation. Moreover, there is a clear one-to-one correlation between λ (HOQWS) and HOQWS including the same beating pattern at $N=17$ ML. These results demonstrate that QSE exists not only in the QWS but also affects the extent of the electron wave functions at the surface. On the other hand, λ derived from the overall electronic states [triangles in Fig. 2(b)] has a rather weak QSE. Furthermore, we see that Si substrate introduces a 1 ML overall phase shift without changing the magnitude of either λ or QWS. Hence, the qualitative conclusions obtained without the substrate can be justified.

As discussed earlier, $\bar{\Gamma}$ valley has the maximum QSE. As such, the even-odd oscillation in the measured LWF could be an order of magnitude larger than the one calculated without including the symmetry-dependent decay. To illustrate this,

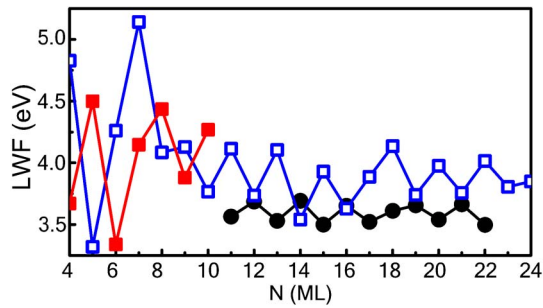


FIG. 3. (Color online) Calculated $\bar{\Gamma}$ -only LWF for free standing (open squares) and Si-supported (solid squares) Pb films as a function of N . For comparison, measured LWF from STS (solid circles) from Refs. 14 and 15 are also shown.

we note that in the STS experiment, the measured LWF is given by $\phi_{\text{LWF}} = 0.952[d(\ln I)/dz]^2$,¹⁶ where I is the tunneling current and z is the distance from the surface. From the Tersoff–Hamann theory,²⁰ tunneling current I is determined by $\rho(z)$ at the STS tip site. As an approximation, we replace $d(\ln I) \equiv dI/I$ in the above expression by $d\rho/\rho \equiv d(\ln \rho)$. To calculate $\rho(z)$, we integrate the electronic states from $E_F - V$ to E_F , where $V = 2$ V is the experimentally applied bias.^{14,15} The electric field effect to the tunneling current is included by applying an electrostatic potential accordingly. Using the asymptotic decay formula for $\rho(z)$, we obtain $\phi_{\text{LWF}} \equiv 0.952/\lambda^2$. Figure 3 shows the LWF calculated by using $\lambda(\bar{\Gamma})$ without (open squares) and with (solid squares) silicon substrate. Quantum oscillation of the LWF can be readily seen. In particular, the magnitude of the oscillation is in the range of hundred meV even when $N = 24$ ML. These results agree with the measured LWF, showing 100 meV magnitude oscillations at $N = 35$ ML.^{14,15} Moreover, when taking into account the 1 ML phase shift due to the substrate, the beating position at $N = 17$ ML also agrees with experiment ($N = 18$ ML). The agreement between theory and experiment suggests that the slow decay of the $\bar{\Gamma}$ states acts as a filter to eliminate the effects of other lower-symmetry states.

In summary, first-principles calculations reveal that QSE affects not only the QWS but also the decay of the electronic states at surfaces. The dependence of the decay on wavevectors further explains the unexpectedly large QSE in the LWF measured by STS. In p -electron systems such as the Pb films,

QSE is strongly symmetry dependent, and the consequence shows up in near-field experiments due to the slow decay of the states with maximum QSE. For s and d electron systems, it can be expected that different states of different symmetries and atomic origins intersect at the Fermi level to induce qualitatively different QSE from that of p -electron systems.

W.X.L. was supported by NSFC (Grant Nos. 20503030 and 20733008) and MOST (Grant No. 2007CB815205). S.B.Z. was supported by DOE/BES under Contract No. DE-AC36-99GO 10337. X.L. was supported by startup fund from DLUT (Grant No. 2007009).

- ¹W. D. Knight, K. Clemenger, W. A. de Heer, W. A. Saunders, M. Y. Chou, and M. L. Cohen, *Phys. Rev. Lett.* **52**, 2141 (1984).
- ²W. B. Su, S. H. Chang, W. B. Jian, C. S. Chang, L. J. Chen, and T. T. Tsong, *Phys. Rev. Lett.* **86**, 5116 (2001).
- ³K. Budde, E. Abram, V. Yeh, and M. C. Tringides, *Phys. Rev. B* **61**, R10605 (2000).
- ⁴V. Yeh, L. Berbil-Bautista, C. Z. Wang, K. M. Ho, and M. C. Tringides, *Phys. Rev. Lett.* **85**, 5158 (2000).
- ⁵N. Binggeli and M. Altarelli, *Phys. Rev. Lett.* **96**, 036805 (2006).
- ⁶M. Hupalo and M. C. Tringides, *Phys. Rev. B* **65**, 115406 (2002).
- ⁷J. J. Paggel, T. Miller, and T. C. Chiang, *Science* **83**, 1709 (1999).
- ⁸Y. Guo, Y. F. Zhang, X. Y. Bao, T. Z. Han, Z. Tang, L. X. Zhang, W. G. Zhu, E. G. Wang, Q. Niu, Z. Q. Qiu, J. F. Jia, Z. X. Zhao, and Q. K. Xue, *Science* **306**, 1915 (2004).
- ⁹P. Czoschke, H. Hong, L. Basile, and T. C. Chiang, *Phys. Rev. Lett.* **93**, 036103 (2004).
- ¹⁰T. L. Chan, C. Z. Wang, M. Hupalo, M. C. Tringides, and K. M. Ho, *Phys. Rev. Lett.* **96**, 226102 (2006).
- ¹¹Y. Jia, B. Wu, H. H. Weitering, and Z. Zhang, *Phys. Rev. B* **74**, 035433 (2006).
- ¹²Y. F. Zhang, J. F. Jia, T. Z. Han, Z. Tang, Q. T. Shen, Y. Guo, Z. Q. Qiu, and Q. K. Xue, *Phys. Rev. Lett.* **95**, 096802 (2005).
- ¹³C. M. Wei and M. Y. Chou, *Phys. Rev. B* **66**, 233408 (2002).
- ¹⁴X. C. Ma, P. Jiang, Y. Qi, J. F. Jia, Y. Yang, W. H. Duan, W. X. Li, X. H. Bao, S. B. Zhang, and Q. K. Xue, *Proc. Natl. Acad. Sci. U.S.A.* **104**, 9204 (2007).
- ¹⁵Y. Qi, X. C. Ma, P. Jiang, Sh. H. Ji, Y. Sh. Fu, J. F. Jia, Q. K. Xue, and S. B. Zhang, *Appl. Phys. Lett.* **90**, 013109 (2007).
- ¹⁶G. Binnig, N. Garcia, H. Rohrer, J. M. Soler, and F. Flores, *Phys. Rev. B* **30**, 4816 (1984).
- ¹⁷B. Hammer, L. B. Hansen, and J. K. Norskov, *Phys. Rev. B* **59**, 7413 (1999).
- ¹⁸J. P. Perdew, J. A. Chevary, S. H. Vosko, K. A. Jackson, M. R. Pederson, D. J. Singh, and C. Fiolhais, *Phys. Rev. B* **46**, 6671 (1992).
- ¹⁹H. J. Monkhorst and J. D. Pack, *Phys. Rev. B* **13**, 5188 (1976).
- ²⁰J. Tersoff and D. R. Hamann, *Phys. Rev. B* **31**, 805 (1985).